

# A Simple Simulation of Surface Plasmon Resonance in The Kretschmann Configuration Using Google Sheets

N. K. Quang<sup>1\*</sup>, N. P. Q. Anh<sup>1</sup>, H. C. Hieu<sup>2</sup>

<sup>1</sup>Faculty of Electronics, Electrical Engineering, and Material Technology,  
University of Sciences, Hue University, Vietnam

<sup>2</sup>Faculty of Physics, VNU University of Science, Vietnam

Received: 03 June 2020. Accepted: 09 October 2020. Published: December 2020

## Abstract

This article describes a simple numerical simulation of three-layer surface plasmon resonance (SPR) in the Kretschmann configuration. The calculation was performed in Google Sheets, a web-based spreadsheet environment that functions similarly to Microsoft Excel where it is easily accessible for students via the internet. Specifically, Fresnel's equations were utilized to calculate the intensity of the reflected light for the p-polarized incident light on a three-layer system. The complex functions were utilized to plot the SPR curves. We examined the change of the resonance angle by the influence of the incident wavelength. The simulation was also performed for different thicknesses of the gold film layer. To demonstrate the sensitivity, we obtained the SPR curves with the variation of the refractive index in the sensitive medium. The SPR accuracy was analysed by comparing our obtained result with the published work. It is intended to incorporate into undergraduate instrumental analysis courses.

**Key words:** google sheets, surface plasmon resonance; kretschmann configuration

## INTRODUCTION

Nowadays, the development of simulation software allows us to model the physical phenomena in more detail. In the physics courses (Abell & Braselton, 2009; Driscoll, 2009), there are various computational tools which allow students to carry out the analysis. Performing interactive simulations of the physical phenomena behind lectures are necessary to enhance and expand the visualization of students in learning, especially in schools where the modern devices may not be available for experimental measurement (Uddin, Ahsanuddin & Khan, 2017; Singh, Khun & Kaur, 2018; Oliveira & Napoles, 2010; Adhi, Sismanto & Setiawan, 2019).

Surface plasmon resonance is one of the optical measurement methods that have been used in modern laboratories for biological and chemical applications (Tang, Zeng & Liang, 2010).

Although the basic knowledge is easy to understand, such devices are relatively scarce because of the cost of the instrument as well as the maintenance process (Tang, Zeng & Liang, 2010; Lavine, Westover, Oxenford, Mirjankar & Kaval, 2007). Furthermore, from the theoretical point of view, several structural parameters could affect the performance of the device, like the effect of wavelength, the prism, and the film materials (Brahmachari & Ray, 2013; Fotana, 2006). To overcome this issue, a theoretical approach is considered as an appropriate strategy. In doing so, numerous papers have proposed theoretical modeling of SPR biosensor based on the Kretschmann configuration (Widayanti & Abraha, 2016; Verma, Gupta, RajanJh, 2011; Maurya, Prajapati & Tripathi, 2018; Bhavsar & Prabhu, 2019; Dai et al., 2019; Zhao et al., 2018). However, most of the works (Brahmachari & Ray, 2013; Sadowski, Korhonen & Pelttonen, 1995; Sarid & Challener, 2010) done in the formulation and analysis of SPR was employed

\*Correspondence Address:  
77 Nguyen Hue, Hue City, Vietnam  
E-mail: nkquang@hueuni.edu.vn

specialized software. This report describes an easy method to utilize the free spreadsheets, Google Sheets, to simulate the SPR in the Kretschmann configuration (https://www.google.com/sheets).

## METHOD

### Background information

Surface plasmon resonance is a phenomenon, in which the electromagnetic waves could be confined to propagate along the interface between two media. In principle, if a p-polarized electric field (external light field) impinges on a metallic surface, there will be a driving force on the free

charges towards the interface and collective oscillations of the quasi-free conduction electrons are excited. In metal, the electrons are nearly free and the collective oscillations of free electrons are called plasmon (Novotny & Hecht, 2012). The coupling of the electron oscillation with the electric field results in the optical wave confined at the surface.

Let us consider the simple model as depicted in Figure 1 (a) where the localized electric field propagate at the interface between metal and air. The existence of the surface plasmon wave at the interface between air and metal can be expressed (Novotny & Hecht, 2012)

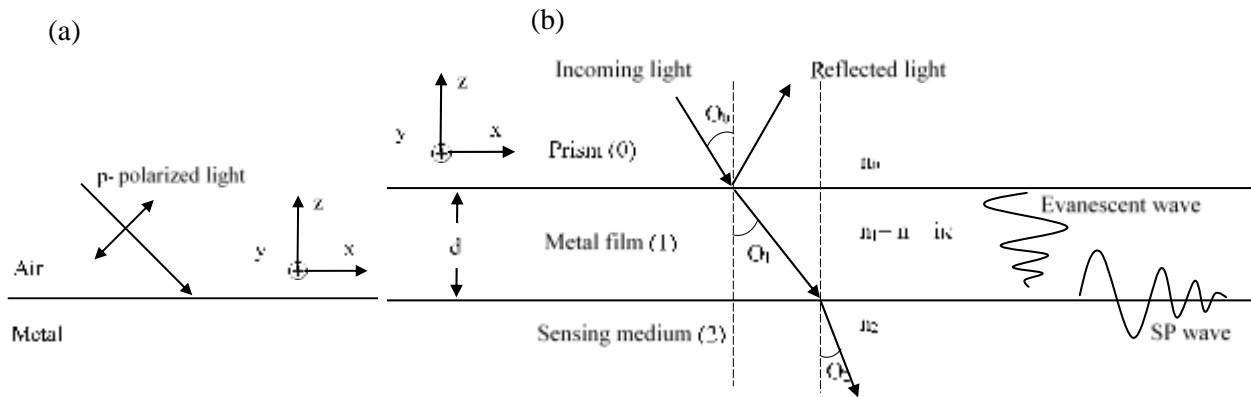


**Figure 1.** (a) A p-polarized light impinges on the interface. (b) Kretschmann configuration for surface plasmon excitation at metal/sensing medium interface.

$$\vec{E}_i = \begin{pmatrix} E_{j,x} \\ 0 \\ E_{j,z} \end{pmatrix} e^{ik_x x - i\omega t} e^{ik_{j,z} z}, j = 1, 2 \quad (1)$$

where  $c$  is the speed of light,  $\omega$  is the light frequency. The obtained wave vector indicates (Novotny & Hecht, 2012)

$$k_x = \frac{\omega}{c} \sqrt{\frac{\epsilon_1 \epsilon_2}{\epsilon_1 + \epsilon_2}}. \quad (2)$$

In general, the dielectric function of metal include the real part and imaginary part, or

$$\epsilon_2 = \epsilon_2' + i\epsilon_2''. \quad (3)$$

We then logically introduce a complex wave-number

$$k_x = k_x' + ik_x''. \quad (4)$$

Substituting the results into equation (1) gives

$$\vec{E}_i = \begin{pmatrix} E_{j,x} \\ 0 \\ E_{j,z} \end{pmatrix} e^{(ik_x' - k_x'')x - i\omega t} e^{ik_{j,z} z}, j = 1, 2. \quad (5)$$

Clearly, the real part  $k_x'$  describes the surface plasmon (SP) wave while the imaginary  $k_x''$  shows the damping of the SP wave propagating along the x-direction. In principle, to maintain the plasmon wave, the imaginary part  $k_x''$  of materials supporting plasmon resonance should have a small value. Later we will take into account this physical origin to explain a dip in the reflectivity curves.

Theoretically, the wave vector of the SP wave at the interface between metal and air does

not match with that of the external coming light (Sarid & Challener, 2010; Novotny & Hecht, 2012). Therefore, SP excitation could not be active if we simply hit the metal surface by the incoming light. To match these two wave vector components for SPR, we have to exploit some special methods (Sarid & Challener, 2010; Novotny & Hecht, 2012).  $\theta_0$  Normally, a prism coupler is employed to achieve the phase matching between the SP wave and excitation wave. By coating a thin metal film on the prism as shown in Figure 1 (b), we can shift the wave vector of the coming photon toward that of the surface plasmon wave (Sarid & Challener, 2010). This method is called the Kretschmann configuration (Raether, 1988). The intensity of the reflected beam is then detected by irradiating light into the prism. The minimum angle appearing on the angle-dependent curve is the resonance angle. Since the shape and the resonance angle of the

SPR curve are extremely sensitive to a change in the refractive index of sensing medium, this technology has been employed as optical sensing technology, even at molecular interaction level (Chen et al., 2007; Shank-Retzlaff & Sligar, 2000).

The theoretical approach performed in research of Raether (1988) and Yamamoto (2010) was used to obtain the reflectivity  $R$ . It is defined by the Fresnel's equations as

$$R = |r_{012}^p|^2 = \left| \frac{r_{01p} + r_{12p} e^{i2\beta}}{1 + r_{01p} r_{12p} e^{i2\beta}} \right|^2 \quad (6)$$

Where  $\beta$  is the phase angle, and  $r_{01p}$  and  $r_{12p}$  are the Fresnel reflection coefficients at the 0-1 and 1-2 interfaces for the p-polarization, respectively. Details of these coefficients are listed in Table 1.

**Table 1.** Details of these terms used in equation (6) and corresponding commands used in Google Sheets

Cell	Term	Description	Command
A3	$\theta_0$	Incident angle in degree	=A2+\$O\$5
B2	$\cos \theta_0$		=COS(RADIANS(A2))
C2	$\sin \theta_1 = \frac{n_0 \sin \theta_0}{n_1}$	Calculate the sine of $\theta_1$ as depicted in figure 1(b)	=IMDIV(\$M\$2*SIN(RADIANS(A2)),COMPLEX(\$N\$2,\$O\$2))
D2	$\cos \theta_1 = \sqrt{1 - (\sin \theta_1)^2}$		=IMSQRT(IMSUB(1,IMPOWER(C2,2)))
E2	$\sin \theta_2 = \frac{n_0 \sin \theta_0}{n_2}$	Calculate the sine of $\theta_2$ as depicted in figure 1(b)	=(M\$2*SIN(RADIANS(A2)))/P\$2
F2	$\cos \theta_2 = \sqrt{1 - (\sin \theta_2)^2}$		=IMSQRT(IMSUB(1,IMPOWER(E2,2)))
G2	$r_{01p} = \frac{n_1 \cos \theta_0 - n_0 \cos \theta_1}{n_1 \cos \theta_0 + n_0 \cos \theta_1}$	The Fresnel reflection coefficient at the 0-1 interface for the p polarization	=IMDIV(IMSUB(IMPRODUCT(COMPLEX(\$N\$2,\$O\$2),B2),IMPRODUCT(\$M\$2,D2)),IMSUM(IMPRODUCT(COMPLEX(\$N\$2,\$O\$2),B2),IMPRODUCT(\$M\$2,D2)))
H2	$r_{12p} = \frac{n_2 \cos \theta_1 - n_1 \cos \theta_2}{n_2 \cos \theta_1 + n_1 \cos \theta_2}$	The Fresnel reflection coefficient at the 1-2 interface for the p polarization	=IMDIV(IMSUB(IMPRODUCT(P\$2,B2),IMPRODUCT(COMPLEX(\$N\$2,\$O\$2),F2)),IMSUM(IMPRODUCT(\$P\$2,D2),IMPRODUCT(COMPLEX(\$N\$2,\$O\$2),F2)))

I2	$\beta = 2\pi \left( \frac{d}{\lambda} \right) n_1 \cos \theta_1$	The phase angle	=IMDIV(IMPRODUCT(2,PI()),\$M\$8,COMPLEX(\$N\$2,\$O\$2),D2),\$N\$8)
J2	$e^{i2\beta}$		=IMEXP(IMPRODUCT(2,COMPLEX(0,1),I2))
K2	$\text{Re } f = \frac{r_{01} + r_{12} e^{i2\beta}}{1 + r_{01} r_{12} e^{i2\beta}}$	Total reflected amplitude R	=IMDIV(IMSUM(G2, IMPRODUCT(H2,J2)),IMSUM(1,IMPRODUCT(G2,H2,J2)))
L2	$R =  \text{Re } f ^2$	The reflectivity R is given by the square of the absolute value of total reflected amplitude $\text{Re } f$	=VALUE(IMPOWER(IMABS(K2),2))

### Students' activities

Obviously, we can see that these terms shown in Table 1 are almost complex numbers, meaning that the complex functions are used for calculating the reflection intensity of the p-polarized light. After completing the theoretical introduction, together with students teacher should briefly introduce the description and syntax of these functions as shown in Table 2. Students then progress to simulate the three-layers SPR based on equation (6) as the following four points: 1) Sign in Google or Gmail account on the web browser. 2) Create a new blank spreadsheet. 3) Carefully type

these terms used in reflectivity equation into each cell as explicitly written in Table 1. As we can see the detail commands for the numerical calculation could be entered wrongly. Therefore the teacher should carefully check during their performance. After finalizing, these cells might not need to change during the calculation. 4) Input appropriate values of the incident wavelength, the refractive indexes of materials and thicknesses of gold as explained in Table 3. These terms could be changed when students execute the simulation. The indices of refraction at several wavelengths were shown in Table 4.

**Table 2.** The description and syntax of these functions used for numerical simulation

Function Syntax	Arguments	Description
=COMPLEX (x, y)	x- The real number y - The imaginary number	Creates a complex number with given real and imaginary coefficients.
=IMSUB (inumber1, inumber2)	inumber1 - Complex number 1 inumber2 - Complex number 2	Gets difference between two complex numbers
=IMSUM (inumber1, [inumber2], ...)	inumber1 - Complex number 1 inumber2 - Complex number 2	Gets sum of complex numbers
=IMDIV(inumber1,inumber2)	inumber1 - Complex number 1 inumber2 - Complex number 2	Returns one complex number divided by another
=IMSQRT( inumber )	inumber - A complex number	Calculates the square root of a complex numbers
=IMPOWER (inumber, number)	inumber - A complex number number - Power to raise number	Raises complex number to given power
=IMEXP( inumber )	inumber - A complex number	Returns the exponential of a complex number
=IMABS (inumber)	inumber - A complex number	Gets absolute value of a complex number

**Table 3.** Description of the data is inputted in the cells

Cell	Description
M2	Refractive index of prism materials which depends on the wavelength of light
N2	The real part of the refractive index of metal
O2	The imaginary of the refractive index of metal
P1	Refractive index of sensing medium
M5	Initial angle of incidence
N5	Final angle of incidence
O5	Increment of angle
M8	Thickness of metal film
N8	Wavelength of incident light

**Table 4.** List of parameters used to calculate the SPR curves

Materials	Refractive index	Dielectric function	Wavelength
Gold film-Au	0.18377 + i3.4313	-11.740 + i1.2611	632.8 nm
Gold film-Au	0.15352 + i4.9077	-24.061 + i1.5068	800 nm
Gold film-Au	0.13100 + i4.0624	-16.486 + i1.0643	700 nm
Gold film-Au	0.24873 + i3.0740	-9.3875 + i1.5292	600 nm
Gold film-Au	0.97112 + i1.8737	-2.5676 + i3.6391	500 nm
Gold film-Au	0.41684 + i1.9530	-1.6580 + i5.7354	400 nm
Prism-SF10	1.7231	2.9692	632.8nm
Prism-SF10	1.7113	2.9285	800 nm
Prism-SF10	1.7174	2.9493	700 nm
Prism-SF10	1.7267	2.9816	600 nm
Prism-SF10	1.7432	3.0386	500 nm
Prism-SF10	1.7783	3.1622	400 nm

The indices of refraction were quoted from <https://refractiveindex.info/>.

## RESULT AND DISCUSSION

Before starting the simulation process, we consider the performance of the spreadsheet. Recall the work done by Masahiro Yamamoto, the reflection curve obtained by SPR sensor consisting of SF10 ( $n = 1.723$ )/gold (50 nm,  $n_1 = 0.1726 + i3.4218$ )/air ( $n = 1.0$ ) for He-Ne laser light (633 nm) presented the resonance angle of about  $37.45^\circ$ . For the comparison, we simulated the three-layers SPR in the same condition of the structural parameters. In Figure 2, the SPR curve indeed confirms the accuracy of the spreadsheet. From the consistency between the calculation and reference (Yamamoto, 2010), the results below were done based on the setup program in which glass prism is SF10 for all the calculations.

### Effect of the incident wavelength

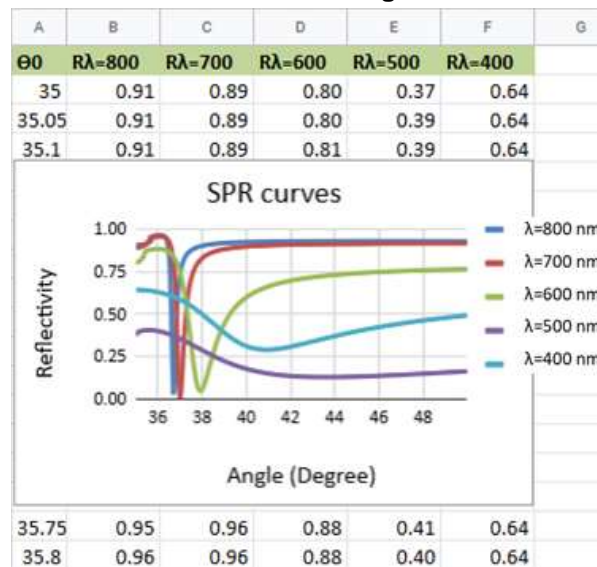


**Figure 3.** The reflection curves of 50 nm thick gold film for different incident wavelengths at 800 nm, 700 nm, 600 nm, 500 nm, and 400 nm, respectively

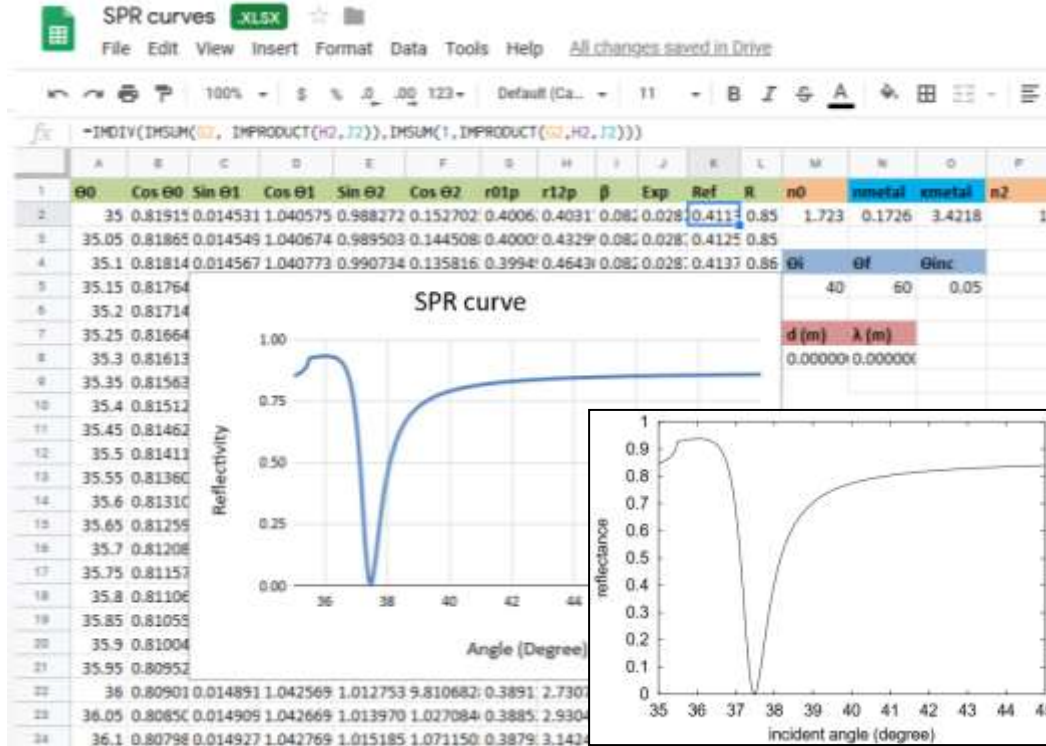


**Figure 2.** The reflection curve obtained by SPR sensor consisting of SF10 ( $n = 1.723$ )/gold (50 nm,  $n_1 = 0.1726 + i3.4218$ )/air ( $n = 1.0$ ) for He-Ne laser light (633 nm). Insert image displays the reflection curve in the same condition of the structural parameters of Yamamoto’s work. Reprinted with permission from (Yamamoto, 2010). Copyright 2002 The Polarographic Society of Japan.

Figure 3 shows the obtained simulation of the SPR curves of 50 nm thick gold film for for different wavelengths at 800 nm, 700 nm, 600 nm, and 500 nm, respectively. The SPR curves of the calculation data reveal the angular dependence of the reflectivity. Namely, gold supports narrow SPR curves for wavelengths greater than 600 nm while the resonance angle broadens significantly for the others. Let us consider the data in Table 4. Here, the imaginary part of a dielectric function at a short wavelength is larger than that at long wavelength. Furthermore, as pointed out in equation (5),  $k_x''$  naturally emerges as the dielectric function of metal includes the imaginary part. Thus, increasing  $\epsilon_2''$  tentatively corresponds to increasing  $k_x''$ , thereby damping the SP wave and no obvious SPR observation (Sarid & Challener, 2010; Novotny & Hecht, 2012; Raether, 1988).

**Effect of the film thicknesses**

To couple the incident light to the SP propagating along the metal/sensing medium interface, adjusting the thickness of the metal film is critical. Normally, the optimal thickness depends on excitation wavelength and materials (Homola, 2006). There are two physical candidate origins we should consider, including radiation damping and the decay of the electric field. As perceived in equation (5), the wave vector  $k_{j,z}$  can be considered in the same way as  $k_x$  where its imaginary part reflecting the evanescent wave created at the interface. Thus, if the metal film thickness exceeds a given value, the evanescent wave is not able to penetrate through it to reach the metal/sensing medium interface for SP excitation (Novotny & Hecht, 2012). In the case of the thin film value, the SP wave oscillating at the interface between metal and sensing medium will be damped due to the

\*Correspondence Address:  
77 Nguyen Hue, Hue City, Vietnam  
E-mail: nkquang@hueuni.edu.vn

prism above as shown in Figure 1 (b) (Novotny & Hecht, 2012).

Following the representation of Figure 4, we could see that the thickness significantly affects the shape of the SPR curve. For a gold film excited at wavelength of 632.8 nm, the strongest excitation of SP appears about 50 nm, in which the reflectivity minimum is nearly zero. Here, the depth of the reflectivity dip at a thickness of 60 nm shows a larger value compared with that of 50 nm. However, the width of the reflectivity was broadened at 60 nm, implying the attenuation of the surface plasmon (Homola, 2006). Consequently, the gold film thickness is limited by an optimal value in the Kretschmann configuration (Fontana, 2006).

**Effect of the change of the refractive index in sensing medium**

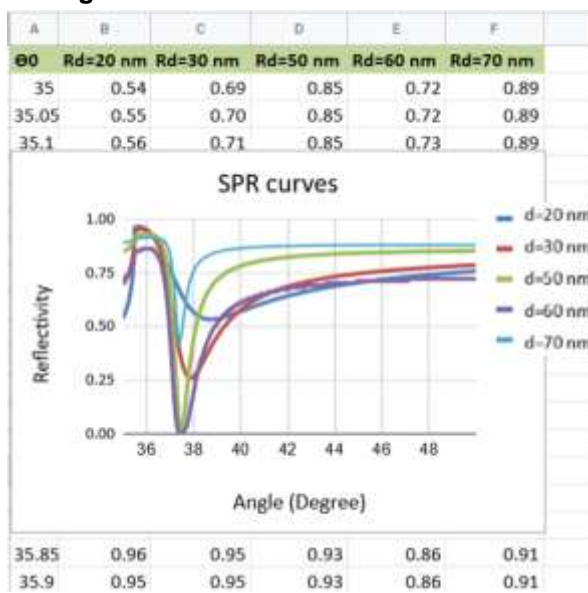


**Figure 4.** The reflection curves of 632.8 nm incident wavelengths for different gold film thicknesses at 20 nm, 30 nm, 50 nm, 60 nm and 70 nm, respectively.

Finally, to demonstrate the sensitivity of this configuration, we further simulate the angle shift due to the change of the refractive index in sensing medium which usually assumed to be caused by biological or chemical reactions (Verma, Gupta & RajanJh, 2011; Dai et al., 2019). Consider that the change in refractive index ( $\Delta n_2 = 0.005$ ) results from the adsorption of biomolecules, the

obtained two SPR curves in Figure 5 indicated an angular shift of  $0.25^\circ$  ( $\Delta\theta = 0.25^\circ$ ) (Verma, Gupta & RajanJh, 2011). We must emphasize that although there is an insignificant change of the refractive index but a strongly shifted plasmon resonance curve can be observed. The reason for the word ‘strongly’ is that the high precision rotation stages allow us to probe such kind of small angle shift without difficulty ([https://www.thorlabs.com/navigation.cfm?guide\\_id=2175](https://www.thorlabs.com/navigation.cfm?guide_id=2175)).

We should also introduce the sensitivity definition of the sensor as (Verma, Gupta & RajanJh, 2011)

$$S = \frac{\Delta\theta}{\Delta n} = \frac{\theta(n_2 + \Delta n) - \theta(n_2)}{\Delta n} \quad (7)$$

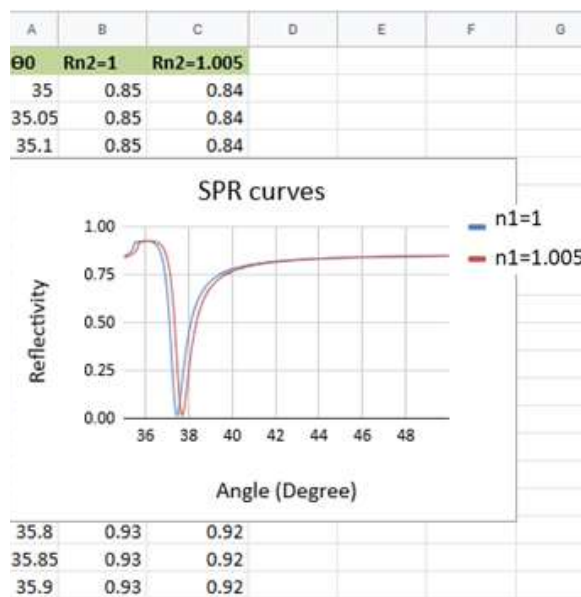


**Figure 5.** The reflection curves wavelength. Refractive indexes of sensing of 50 nm gold thin film for 632.8 nm incident medium are 1 and 1.005, respectively.

Here,  $\Delta\theta$  is the shift of resonance angle corresponding to the change of the refractive index  $\Delta n$  in the sensing medium. To enrich the visualization of students, a further assignment could give, in which the teacher might ask each student to do their simulation with different noble metals of the thin film. The results then can be used to compare the sensitivity of the sensor between gold metal

and other materials. For a more advanced level, students could expand the scope by using the calculation process applied for multi-layered systems as mentioned in works of (Fujiwara, 2007; Azzam & Bashara (1977).

## CONCLUSION

The calculation in this work is an interdisciplinary subject between the physical phenomenon and instrumental analysis. With a simple performance, we intend at providing an easy method to use Google Sheets for the simulation of three-layer SPR in the Kretschmann configuration. In class, without using any numerical simulation other than a personal computer connected to the internet, the students still can visualize the performance of three layers SPR sensor that they might have no chance to experience the device. Thus, this presentation aims to provide students an overview of the SPR concept, which could be served as a module on instrumental analysis of laboratory classes comprised of the optics-based methods.

## REFERENCES

- Abell, M. L. L. & Braselton, J. P. (2009). *Mathematica by Example*. Academic Press.
- Adhi, A., Sismanto & Setiawan, A. (2019). Invers Modeling Gravity Data for Semi-Infinite Slab Using Matlab. *Jurnal Pendidikan Fisika Indonesia* 15 (2) (2019) 107-113. <https://doi.org/10.15294/jpfi.v15i2.21937>.
- Azzam, R. M. A. & Bashara, N. M. (1977). *Ellipsometry and Polarized Light*, North Holland.
- Bhavsar K. & Prabhu, R. (2019). Investigations on sensitivity enhancement of SPR biosensor using tunable wavelength and graphene layers. *IOP conference Series: Materials Science and Engineering*, 499, 012008. <https://doi.org/10.1088/1757-899X/499/1/012008>.
- Brahmachari, K. & Ray, M. (2013). Effect of prism material on design of surface plasmon resonance sensor by admittance loci method. *Frontiers of Optoelectronics*, 6, 185-193. <https://doi.org/10.1007/s12200-013-0313-2>.
- Chen, H., Lee, L., Choi, S., Kim, J.-H., Choi, H.-J., Kim S.-H., Lee J., & Koh K. (2007). Comparative study of protein immobilization properties on Calixarene monolayers. *Sensors*, 7 (7), 1091-1107. <https://doi.org/10.3390/s7071091>.
- Dai, X., Liang, Y., Zhao, Y., Gan, S., Jia, Y., & Xiang, Y. (2019). Sensitivity enhancement of a surface plasmon resonance with Tin Selenide (SnSe) allotropes. *Sensors*, 19 (1), 172. <https://doi.org/10.3390/s19010173>.
- Driscoll, T. A. (2009). *Learning MATLAB*. Society for Industrial and Applied Mathematics.
- Fontana, E. (2006). Thickness optimization of metal films for the development of surface-plasmon-based sensors for nonabsorbing media. *Applied Optics*, 45 (29), 7632-7642. <https://doi.org/10.1364/AO.45.007632>.
- Fujiwara, H. (2007). *Spectroscopic Ellipsometry: Principles and Applications*, Wiley.
- Homola, J. (2006). *Surface Plasmon Resonance Based Sensors*. Springer. <https://refractiveindex.info/>. <https://www.google.com/sheets/about/>. [https://www.thorlabs.com/navigation.cfm?guide\\_id=2175](https://www.thorlabs.com/navigation.cfm?guide_id=2175)
- Lavine, B. K., Westover, D. J., Oxenford, L., Mirjankar, N., & Kaval, N. (2007). Construction of an inexpensive surface plasmon resonance instrument for use in teaching and research. *Microchemical Journal*, 86 (2), 147-155. <https://doi.org/10.1016/j.microc.2007.02.003>.
- Maurya, J. B., Prajapati, Y. K., & Tripathi, R. (2018). Effect of molybdenum disulfide layer on surface plasmon resonance biosensor for the detection of bacteria. *Silicon*, 10 (2), 245-256. <https://doi.org/10.1007/s12633-016-9431-y>.
- Novotny, L. & Hecht, B. (2012). *Principles of Nano-Optics*, Cambridge University Press.
- Oliveira, M. C. & Nápoles, S. (2010). Using a spreadsheet to study the oscillatory movement of a mass-spring system. *Spreadsheets in Education*, 3 (3), 2. Retrieved from <https://sie.scholasticahq.com/article/4563>.
- Raether, H. (1988). *Surface Plasmons on Smooth and Rough Surfaces and on Gratings*, Springer.
- Sadowski, J. W., Korhonen, I. K. J. & Peltonen, J. P. K. (1995). Characterization of thin films and their structures in surface plasmon resonance measurements. *Optical Engineering*, 34 (9), 2581-2586. <https://doi.org/10.1117/12.208083>.
- Sarid, D. & Challener, W. A. (2010). *Modern Introduction to Surface Plasmons: Theory, Mathematical Modeling, and Applications*, Cambridge University Press.
- Shank-Retzlaff, M.-L. & Sligar, S. G. (2000). Analyte gradient-surface plasmon resonance: a one-step method for determining kinetic rates and macromolecular binding affinities. *Analytical Chemistry*,

- 72 (17), 4212-4220. <https://doi.org/10.1021/ac0001030>.
- Singh, I., Khun, K. K. & Kaur, B. (2018). Simulating Fraunhofer diffraction of waves using Microsoft excel spreadsheet. *Physics Education*, 53, 055010. <https://doi.org/10.1088/1361-552/aacd82>.
- Tang, Y., Zeng X., & Liang, J. (2010). Surface plasmon resonance: an introduction to a surface spectroscopy technique. *Journal of Chemical Education*, 87 (7), 742-746. <https://doi.org/10.1021/ed100186y>.
- Uddin, Z., Ahsanuddin, M. & Khan, D. A. (2017). Teaching physics using Microsoft excel. *Physics Education*, 52, 053001. <https://doi.org/10.1088/1361-6552/aa7919>.
- Verma, R, Gupta, B. D., & RajanJh (2011). Sensitivity enhancement of a surface plasmon resonance based biomolecules sensor using graphene and silicon layers. *Sensor and Actuators*, 160 (1), 623-631. <https://doi.org/10.3390/s20010131>.
- Widayanti & Abraha, K. (2016). Study on the effect of nanoparticle bimetallic coreshell Au-Ag for sensitivity enhancement of biosensor based on surface plasmon resonance. *Journal of Physics: Conference Series*, 694, 012075. <https://doi.org/10.1088/1742-6596/694/1/012075>.
- Yamamoto, M. (2010). Surface plasmon resonance (SPR) theory: tutorial. *J-STAGE*, 48 (3), 209-237. <https://doi.org/10.5189/revpolarography.48.209>.
- Zhao, X., Huang, T., Ping, P. S., Wu, X. Huang, Pan, J. Cheng, P. (2018). Sensitivity enhancement in surface plasmon resonance biochemical sensor based on transition metal dichalcogenides/graphene heterostructure. *Sensors*, 18 (7), 2056. <https://doi.org/10.3390/s18072056>.